Coupled control of land uses and aquatic biological processes on the diurnal hydrochemical variations in the five ponds at the Shawan Karst Test Site, China: Implications for the carbonate weathering-related carbon sink

Bo Chen [a,b], Rui Yang [a], Zaihua Liu [a,*], Hailong Sun [a], Hao Yan [a], Qingrui Zeng [a,b], Sibo Zeng [c], Cheng Zeng [a], Min Zhao [a]

[a] State Key Laboratory of Environmental Geochemistry, Institute of Geochemistry, CAS, Guiyang 550081, China
[b] University of Chinese Academy of Sciences, Beijing 100049, China
[c] School of Geographical Sciences, Southwest University, Chongqing 400715, China

ARTICLE INFO

ABSTRACT

High-resolution hydrochemical data from five spring-fed ponds are presented to demonstrate the effect of different land uses and aquatic biological processes on the carbon cycle at a karst-analog test site. The results show that hydrochemical parameters including pH and the concentrations of HCO_3^-, Ca^{2+}, NO_3^-, partial pressures of CO_2 (pCO_2) and dissolved O_2 (DO) as well as carbon isotopic compositions ($\delta^{13}C$) of HCO_3^- in the pond water all displayed distinct diurnal variations, while those of the spring water itself were rather stable. The coupled dynamic behaviors of pCO_2, DO and NO_3^- indicate a significant influence from the metabolism of submerged plants in the ponds. In the afternoon, when photosynthesis is the strongest, the pCO_2 of the five pond waters was lower even than that of the ambient atmosphere, demonstrating the existence of a "biological carbon pumping (BCP) effect", similar to that in the oceans. It was determined that, in October (autumn), the BCP fluxes in the five spring-fed ponds were 156 ± 51 t C km^{-2} a^{-1} in P1 (Pond 1 – adjoining a bare rock shore), 239 ± 83 t C km^{-2} a^{-1} in P2 (adjoining uncultivated soil), 414 ± 139 t C km^{-2} a^{-1} in P3 (adjoining land cultivated with corn), 493 ± 165 t C km^{-2} a^{-1} in P4 (adjoining grassland) and 399 ± 124 t C km^{-2} a^{-1} of P5 (adjoining brushland), indicating the potentially significant role of aquatic photosynthesis in stabilizing the carbonate weathering-related carbon sink. In addition, by comparing the DIC concentrations and fluxes of DIC transformed into autochthonous organic matter (AOC) in the five ponds, the so-called "DIC fertilization effect" was found in which more AOC is produced in pond waters with higher concentrations of DIC. This implies that the carbon cycle driven by aquatic biological processes can be regulated by changing land use and cover, the latter determining the DIC concentrations. Further, the rock weathering-related carbon sink is underestimated if one only considers the DIC component in surface waters instead of both DIC and AOC.

© 2017 Elsevier B.V. All rights reserved.

1. Introduction

Inland freshwater ecosystems, particularly rivers, lakes and reservoirs, can affect regional carbon balances by storing, oxidizing and transporting terrestrial carbon and thus significantly influencing the terrestrial carbon budget (Cole et al., 2007). In earlier previous studies, dissolved inorganic carbon (DIC) transport through rivers into the ocean has been studied extensively; conversion from inorganic to organic carbon as well as the consequent carbon sequestration or release

in freshwater ecosystems (Z. Liu et al., 2010; Y. Liu et al., 2010; Liu and Dreybrodt, 2015), however, is generally overlooked.

Recently, research has shown that autochthonous organic carbon (AOC) from DIC transformation by aquatic photosynthesis is an important part in river transported/buried carbon (Waterson and Canuel, 2008; Yang et al., 2016). Especially in karst basins, due to the rapid carbonate weathering which provides abundant DIC and the aquatic photosynthesis which utilizes DIC as its carbon source, the amount of AOC can be considerable and thus its corresponding contribution to karst-related carbon sinks must be considered (Liu and Dreybrodt, 2015). The karst-related carbon sink is a complex, combined effect including a series of physical, chemical and biological processes, and can be studied by understanding the spatiotemporal hydrochemical variations in the

aquatic ecosystems (De Montety et al., 2011; Liu et al., 2015; Yang et al., 2015). Previous work has emphasized particular aspects of geochemistry or biology in karst waters (Liu et al., 2006, 2008; Parker et al., 2007; Z. Liu et al., 2010, Y. Liu et al., 2010; De Montety et al., 2011; Kurz et al., 2013), even specifically focusing on the influence of submerged plant metabolism (or primary producers) on stream water hydrochemistry, including oxygen dynamic and nutrient cycling (Clarke, 2002; Schulz and Köhler, 2006; Heffernan and Cohen, 2010; Parker et al., 2010; Poulson and Sullivan, 2010). There are also several studies showing that diurnal changes of dissolved organic carbon (DOC) are attributable to daily changes in the productivity levels of aquatic communities (Harrison et al., 2005; Spencer et al., 2007). However, research on the interactions among physical, chemical and biological processes is still lacking, and thus the driving mechanisms remain unclear and need to be further resolved.

It is common that natural karst catchments have mixed vegetation types, making data interpretation difficult, so, an experimental test site, controlling for all variables but one, can help simplify and understand the impact of different land covers on the karst hydrobiogeochemical processes, and improve the quantification of the related carbon budgets. With this requirement in view, five karst spring-pond systems of the same size but with different single types of vegetation cover were constructed at Shawan (Puding County, Guizhou Province, China), to investigate the diurnal hydrochemical variations in the ponds in different seasons. It was found that aquatic metabolism is the major driving force for the daily hydrochemical cycle and even causes strong Biological Carbon Pumping (BCP) effects. Moreover, higher DIC concentrations result in higher aquatic photosynthetic products, which are called "DIC fertilization effects" (Z. Liu et al., 2010; Yang et al., 2016), and indicate, for the first time, that carbon sequestration originating from water-carbonate rock-CO_2 gas-aquatic organism interaction could be regulated by land use and land cover changes, which result in changes in DIC concentrations, and are important to future carbon management in mitigating climate change.

2. Study site

The simulation test site (Fig. 1, 26°14′-26°15′N, 105°42′-105°43′E, 1200 m asl) is located in the Puding Comprehensive Karst Research and Experimental Station, Puding County, Guizhou Province, China. The climate is humid subtropical monsoon with annual mean air temperature of about 15.1 °C and mean annual precipitation of 1315 mm, 80% of which occurs during the rainy season from May to October (Yang et al., 2012).

Five concrete tanks LUCC (Land Use/Cover Change) 1 to LUCC5, each 20 m long and 5 m wide and 3 m deep, coated with epoxy resin to avoid the influence of possible concrete erosion on the tank hydrochemistry, were constructed at the site, filled with 2 m dolomitic limestone rubble in the lower part and topped with 0.5 m soil with the exception of LUCC1, which was left with rubble only. Construction was completed in January 2014. Tank LUCC1, with no soil and plants but only carbonate rubble was used to simulate the land-use condition in karst rocky desert. In Tank LUCC2, there was no induced plant growth but soil and carbonate rubble were used to simulate land-use conditions in bare land. Tank LUCC3 was planted with corn to simulate cultivated land-use. Alfalfa and Roxburgh rose were sown in the soils of Tank LUCC4 and Tank LUCC5 in January 2014 to simulate grass and shrub land-uses respectively (Fig. 1). A drainage hole was cut in each tank to simulate outlet of a karst spring (S1 to S5), which fed into an artificial pond (P1 to P5) with 3 m long, 50 cm wide, and 50 cm deep to simulate influence of groundwater on surface water (Fig. 1). Equal numbers of the locally dominant submerged plants, including Spirogyra, Hornwort and Charophyta, were transplanted in each spring-fed pond in January 2014 to simulate the influence of biological processes on the hydrochemistry of the pond waters.

Fig. 1. Five springs (S1 to S5, upper image) and the spring-fed ponds (P1 to P5, upper and lower image) with flourishing submerged plants and WTW data loggers and the floating chamber. The types of land uses feeding the springs are bare rock land (LUCC1), abandoned bare land (LUCC2), cultivated land (LUCC3), grassland (LUCC4), and shrubland (LUCC5).

3. Methods

3.1. Field monitoring

The field campaigns were conducted under sunny and steady flow conditions for 48 h on 26–28 April, 19–21 July, 24–26 October 2015 and 23–25 January 2016, two diurnal cycles each for spring, summer, autumn and winter respectively. We found similar diurnal hydrochemical variation patterns for all seasons, but highest range for autumn (September to November) and lowest range for winter (December to February). Therefore, for simplification and shortening the paper, we chosen the data for autumn and winter as a highest-lowest contrast to study climate influence on the BCP-effect. Five Manta Multi-parameter Data Logger 2.0 and five WTW Technology Multiline 350i were programmed at each spring vent and pond outlet (Fig. 1), respectively, to collect 15-min interval readings of water temperature (T), pH, electrical conductivity (EC, 25 °C), and dissolved oxygen (DO) for the daily cycles. The meters were calibrated prior to deployment using pH (4, 7 and 10), EC (1412 μs cm^{-1}), and DO (0% and 100%) standards. Resolution of pH, T, DO and EC was 0.01, 0.01 °C, 0.01 mg L^{-1} and 0.01 μS cm^{-1}, respectively. In addition, the flow rate of each spring (L min^{-1}) was measured at the beginning and end of the study periods.

3.2. Sampling and analysis

Two sets of water samples were passed through 0.45 μm Millipore filters into 20 mL acid-washed high-density polyethylene bottles for major cation and anion determination. The cation samples were acidified to pH < 2.0 with concentrated nitric acid to prevent complexation

and precipitation. Concentrations of K^+, Na^+, Ca^{2+} and Mg^{2+} were determined with an inductively coupled plasma optical emission spectrometer (ICP-OES) and Cl^-, NO_3^- and SO_4^{2-} with an ICS-90 ion chromatograph. The experimental detection resolution of these ions was 0.01 mg L^{-1}. In addition, concentration of HCO_3^- was titrated in-situ, using an Aquamerck alkalinity test kit with an estimated accuracy of 0.05 mmol L^{-1} (Yang et al., 2015).

Water samples preserved with 2 mL saturated $HgCl_2$ added solution were first filtered through 2 mm mesh sieve to remove large particles and debris of aquatic plants and then through 0.2 μm Whatman GF/F filter into brown glass bottles which were combusted at 450 °C for 3 h in a Muffle furnace. While DOC entered the bottles with the water, any particulate organic carbon (POC) was captured on the Whatman filters. DOC samples were stored at 4 °C and analyzed by an Analytik Jena N/C Multi3100. POC samples were dried at 65 °C for 48 h and then fumed with concentrated hydrochloric acid in a sealed desiccator for 24 h to remove inorganic carbon. After drying again, the samples were analyzed by Vario MAX CN Elementar with an analytical error less than ± 2%. TOC is composed of DOC and POC, thus the concentration of TOC could be calculated (Suman et al., 2012).

Water samples for carbon isotope composition ($\delta^{13}C_{DIC}$) were collected in pre-cleaned 60 mL glass vials through 0.2 μm Whatman GF/F filter with no air bubbles or headspace. One drop of saturated $HgCl_2$ solution was added to each sample to prevent microbial activity, and all samples were kept at 4 °C until being analyzed by MAT-252 mass spectrometer. The results are reported relative to the V-PDB standard with an uncertainty less than ± 0.03‰ (Sun et al., 2011).

All the water samples were collected once every four hours. In addition, a static floating chamber (size $2.5 \times 0.5 \times 0.1$ m with the area of 1.25 m^2 and the volume of 125 L) was placed on the water surface of each pond to determine the CO_2 exchange flux between water and air three times a day (early morning, noon and evening). Each 20 mL gas sample was pumped from the chamber by a syringe and injected into a 12 mL vacuum glass vial at sampling times of 0, 2, 4, 6, and 8 min after the deployment of the chamber. All gas samples were stored at room temperature and each CO_2 concentration was measured by Agilent-7890 gas chromatography with resolution of 0.01 ppm.

3.3. Estimating CO_2 partial pressure (pCO_2) and saturation index for calcite (SI_C)

pCO_2 and SI_C values were calculated with the PHREEQC3 program (http://wwwbrr.cr.usgs.gov/projects/GWC_coupled/phreeqc/index.html) by entering pH, T and concentrations of seven major ions. Ca^{2+} and Mg^{2+} are the major cations, while HCO_3^- is the dominant counterbalancing anion in these waters, so they dominate EC in these systems. Consequently, continuous concentrations of Ca^{2+}, Mg^{2+}, and HCO_3^- can be estimated from the automatically recorded data of EC (Liu et al., 2007). Based on the titrated [HCO_3^-] as well as analyzed [Ca^{2+}] and [Mg^{2+}], the linear relationships between concentrations of these ions and EC were established as the equations presented in Table 1.

4. Results

The forty-eight hours data for the two diurnal cycles for the springs (S1 to S5) and ponds (P1 to P5) in different seasons (October for autumn, January for winter) are summarized in Tables 2 and 3 and presented graphically in Figs. 2–5.

4.1. Spatio-temporal physicochemical changes in the spring-pond systems

All parameters in the five springs (S1-S5) showed little diurnal variation (Figs. 2 and 3, Tables 2 and 3), with coefficients of variation (CVs) being generally <1% except for SI_C, pCO_2, DO and $\delta^{13}C_{DIC}$. However, some seasonal differences, e.g., higher T, pCO_2 and [HCO_3^-] in autumn than in winter, were noted. In contrast, there were remarkable source differences in the hydrochemical values among the five springs (Figs. 2 and 3, Tables 2 and 3). The pCO_2 and [HCO_3^-] values of the springs showed a descending order from S4 (grass land LUCC4), S3 (cultivated land LUCC3), S5 (brush land LUCC5), S2 (uncultivated land LUCC2) to S1 (bare rock land LUCC1).

In contrast to the springs, there were pronounced diurnal hydrochemical cycles in the spring-fed ponds during autumn monitoring period. Two types of patterns with varying amplitudes were observed on the diurnal timescale: DO and DOC increased during daytime and decreased at night, while pCO_2 and [HCO_3^-] did the opposite (Fig. 4). The pCO_2 and [HCO_3^-] were the highest in P4 while P1 had the lowest values (Fig. 4 and Tables 2 and 3), characteristics inherited from their springs. In addition, the average concentration of DOC in P4 was 4, 3.7, 2.8 and 2.4 times higher than that in P1, P2, P3 and P5, respectively. [NO_3^-] decreased while DO increased during daytime and both reversed at night. Compared to the changes in autumn, the diurnal hydrochemical variations in winter showed similar trends but much smaller ranges (Fig. 5 and Tables 2 and 3). For example, the maximum CV in the pCO_2 in the ponds reached 105.9% in October, while it was only 30.4% in January.

4.2. CO_2 fluxes in the spring-fed ponds

Daily mean fluxes of CO_2 in each pond were estimated from data obtained in the morning, at noon and in the evening (Table 4). It can be seen that CO_2-degassing is the most intense in the morning with the highest flux of 42.9 mg m^{-2} h^{-1} in P3 in autumn, but nearly half of that value in winter. However, in both seasons, there exist obvious negative CO_2 fluxes (from atmosphere to the water) in all ponds at noon, with the most negative value of − 84.3 mg m^{-2} h^{-1} in P3 in the autumn, but an order of magnitude smaller in winter. In the evening the CO_2 fluxes turned to positive again, but were lower than those in the morning.

In addition, the CO_2 fluxes showed significant source differences in the autumn (Table 4). Among these ponds, P1 and P2 have the first and second highest efflux respectively (42.8 and 32.9 mg m^{-2} h^{-1} in the morning, 28.8 and 25.1 mg m^{-2} h^{-1} in the evening) as well as the first and second lowest influx (− 27.6 and − 30.1 mg m^{-2} h^{-1} at

Table 1
Parameters in the equation relating concentrations of Ca^{2+}, Mg^{2+} or HCO_3^- to EC ([Ion concentration] = a*EC + b).

Site		P1		P2		P3		P4		P5	
Month		Oct.	Jan.	Oct.	Jan.	Oct.	Jan.	Oct.	Jan.	Oct.	Jan.
[Ca^{2+}]	a	0.20 ± 0.01	0.19 ± 0.01	0.15 ± 0.02	0.16 ± 0.02	0.18 ± 0.01	0.18 ± 0.02	0.16 ± 0.00	0.16 ± 0.01	0.18 ± 0.01	0.15 ± 0.01
vs EC	b	−7.78 ± 1.34	−6.82 ± 1.22	−0.72 ± 0.16	−0.94 ± 0.35	−3.82 ± 0.74	−5.33 ± 1.18	−0.82 ± 0.09	−0.89 ± 0.10	−4.47 ± 0.92	−0.88 ± 0.02
	r^2	0.85	0.81	0.82	0.80	0.87	0.83	0.90	0.84	0.91	0.86
[Mg^{2+}]	a	0.01 ± 0.00	0.01 ± 0.00	0.04 ± 0.00	0.03 ± 0.00	0.01 ± 0.00	0.01 ± 0.00	0.05 ± 0.00	0.05 ± 0.00	0.02 ± 0.00	0.02 ± 0.00
vs EC	b	6.78 ± 0.10	6.18 ± 0.11	0.20 ± 0.01	0.32 ± 0.04	8.76 ± 0.12	8.13 ± 0.19	0.16 ± 0.01	0.14 ± 0.01	7.12 ± 0.13	6.48 ± 0.15
	r^2	0.76	0.75	0.79	0.79	0.81	0.71	0.75	0.72	0.78	0.73
[HCO_3^-]	a	0.66 ± 0.02	0.63 ± 0.03	0.63 ± 0.02	0.63 ± 0.02	0.61 ± 0.02	0.60 ± 0.03	0.61 ± 0.02	0.62 ± 0.02	0.63 ± 0.02	0.62 ± 0.03
vs EC	b	−7.8 ± 9.5	−5.9 ± 7.6	−4.9 ± 6.7	−4.7 ± 6.8	2.1 ± 4.1	3.2 ± 4.9	4.6 ± 6.5	3.9 ± 5.8	2.7 ± 3.7	3.5 ± 5.6
	r^2	0.88	0.81	0.91	0.89	0.89	0.84	0.87	0.82	0.89	0.85

Table 2
Statistics on the diel variations of physicochemical parameters in the spring-pond systems in the autumn month (October).

Site	S1	S2	S3	S4	S5	P1	P2	P3	P4	P5
T (°C)	20.9–21.0[a]	21.1–21.1	20.8–20.8	20.9–21.0	20.4–20.5	17.0–21.1	20.3–24.9	20.6–24.8	20.5–24.8	20.3–24.3
	(21.0)[b] [0.2][c]	(21.1) [0.1]	(20.8) [0.1]	(20.9) [0.1]	(20.5) [0.2]	(18.5) [6.5]	(22.0) [5.8]	(22.3) [5.7]	(22.2) [5.8]	(22.1) [5.6]
pH	8.2–8.3	7.9–8.0	7.8–7.9	7.5–7.5	7.9–8.0	7.9–9.7	7.9–9.5	7.9–9.3	7.9–8.3	7.6–9.1
	(8.2) [0.1]	(8.0) [0.2]	(7.8) [0.1]	(7.5) [0.0]	(7.9) [0.1]	(8.7) [6.7]	(8.7) [6.2]	(8.6) [5.9]	(7.9) [2.7]	(8.3) [5.1]
EC (µs cm⁻¹)	207.9–208.8	243.7–253.2	246.1–355.0	421.9–424.9	323.6–325.0	162.7–223.0	201.7–234.0	271.0–325.0	364.0–405.0	256.0–312.0
	(208.4) [0.1]	(248.2) [0.8]	(351.1) [0.7]	(423.4) [0.1]	(324.2) [0.1]	(200.8) [9.2]	(217.5) [4.6]	(298.7) [5.6]	(393.0) [2.5]	(284.2) [6.7]
[Ca²⁺] (mg L⁻¹)[d]	30.7–30.8	35.7–37.0	50.0–51.3	60.6–61.0	46.9–47.1	24.3–32.8	29.7–34.3	39.5–47.1	52.5–58.3	37.4–45.2
	(30.7) [0.1]	(36.3) [0.8]	(50.7) [0.6]	(60.8) [0.1]	(47.0) [0.1]	(24.7) [8.7]	(32.0) [4.3]	(43.4) [6.0]	(56.6) [2.4]	(41.4) [6.5]
[Mg²⁺] (mg L⁻¹)[d]	9.7–9.8	10.8–10.9	16.2–16.3	21.0–21.2	12.8–12.9	9.1–9.2	10.8–11.0	14.8–16.9	19.8–21.6	11.6–12.9
	(9.8) [0.1]	(10.9) [0.1]	(16.2) [0.1]	(21.0) [0.1]	(12.8) [0.1]	(9.1) [8.1]	(11.0) [4.1]	(15.9) [5.1]	(21.0) [2.1]	(12.5) [6.1]
[HCO₃⁻] (mg L⁻¹)[d]	118.6–119.2	141.2–147.1	205.7–211.3	253.4–255.3	191.5–192.4	90.1–128.1	114.3–135.0	158.4–192.4	216.9–242.8	148.9–184.2
	(118.9) [0.1]	(144.0) [0.9]	(208.8) [0.7]	(254.4) [0.1]	(191.9) [0.1]	(114.1) [10.2]	(126.6) [5.0]	(175.8) [6.0]	(235.2) [2.6]	(166.7) [7.2]
[SO₄²⁻] (mg L⁻¹)[d]	26.6–26.7	43.2–43.3	35.4–35.5	27.0–27.1	42.6–42.7	24.7–24.8	41.2–41.5	60.4–60.9	26.8–27.2	42.3–43.9
	(26.7) [0.1]	(43.2) [0.1]	(35.4) [0.1]	(27.1) [0.1]	(42.7) [0.1]	(24.7) [0.1]	(41.5) [0.1]	(60.8) [0.1]	(27.1) [0.1]	(43.6) [0.1]
[NO₃⁻] (mg L⁻¹)[e]	3.3–3.4	14.8–14.9	7.3–7.4	0.7–0.8	–	1.7–2.3	11.3–11.9	3.8–4.6	–	–
	(3.4) [0.1]	(14.9) [0.1]	(7.3) [0.1]	(0.7) [0.1]		(2.0) [21.1]	(11.7) [18.9]	(4.2) [15.5]		
SI_C	0.3–0.3	0.2–0.2	0.3–0.4	0.1–0.1	0.4–0.4	0.1–1.4	0.1–1.4	0.3–1.5	0.3–0.8	0.1–1.3
	(0.3) [1.6]	(0.2) [7.2]	(0.3) [1.2]	(0.1) [2.0]	(0.4) [1.4]	(0.6) [66.5]	(0.7) [60.9]	(0.9) [42.9]	(0.5) [36.0]	(0.7) [52.7]
pCO₂ (Pa)	61–63	130–160	265–284	804–828	195–200	1–162	3–167	5–252	113–596	9–426
	(62) [1.1]	(142) [5.1]	(273) [1.6]	(830) [0.6]	(198) [1.1]	(45) [101.8]	(51) [104.1]	(78) [105.9]	(325) [47.9]	(116) [99.7]
DO (mg L⁻¹)	4.1–4.6	3.6–4.6	2.4–3.0	0.0–0.0	0.1–0.5	3.3–13.2	6.7–20.0	3.0–20.0	2.3–14.0	5.0–17.6
	(4.4) [3.4]	(4.0) [4.8]	(2.6) [4.2]	(0.0) [0.0]	(0.2) [71.1]	(6.8) [38.9]	(12.7) [31.2]	(11.8) [43.2]	(7.8) [45.7]	(9.9) [35.5]
DOC (mg L⁻¹)[e]	1.2–1.3	1.2–1.3	2.2–2.3	3.5–3.6	0.8–0.9	1.3–1.8	1.3–1.9	1.7–2.4	5.5–6.1	2.0–2.8
	(1.3) [0.1]	(1.2) [0.1]	(2.2) [0.1]	(3.6) [0.1]	(0.9) [0.1]	(1.5) [9.9]	(1.6) [13.9]	(2.1) [18.2]	(5.8) [11.1]	(2.4) [21.3]
POC (mg L⁻¹)[e]	0.6–0.7	0.5–0.6	0.8–0.9	1.1–1.2	0.2–0.3	0.9–1.4	1.7–2.0	1.6–2.1	1.9–2.4	1.4–1.9
	(0.7) [0.1]	(0.6) [0.1]	(0.9) [0.1]	(1.1) [0.1]	(0.3) [0.1]	(1.3) [5.2]	(1.8) [9.7]	(1.9) [11.3]	(2.2) [8.9]	(1.7) [15.1]
δ¹³C_DIC (‰)[e]	−3.0–2.2	−3.6–3.1	−4.5–4.1	−15.7–15.0	−8.9–9.5	−3.7–1.6	−4.8–2.2	−4.0–2.6	−14.7–13.4	−8.7–6.6
	(−2.6) [7.6]	(−3.3) [3.3]	(−4.3) [3.3]	(−15.4) [1.2]	(−9.7) [1.0]	(−2.5) [27.8]	(−3.7) [25.9]	(−3.1) [14.3]	(−14.1) [3.1]	(−7.6) [8.4]
Q (L min⁻¹)	0.4	0.3	0.3	0.2	0.3	0.4	0.3	0.3	0.2	0.3

The mean values of the other ions: [K⁺] = 1.6 mg L⁻¹, [Na⁺] = 1.6 mg L⁻¹, [Cl⁻] = 0.1 mg L⁻¹, [PO₄³⁻]: lower than the detection limit.
[a] Minimum-maximum.
[b] Mean values, number of samples are 192.
[c] CV or variation coefficients = (standard deviation / mean) %.
[d] Calculated values via Equations.
[e] Sample analyzed value, number of samples are 12 (δ¹³C_DIC samples are 24 in autumn).

Table 3
Statistics on the diel variations of physicochemical parameters in the spring-pond systems in the winter month (January).

Site	S1	S2	S3	S4	S5	P1	P2	P3	P4	P5
T (°C)	12.1–12.9[a]	14.4–14.8	14.9–15.3	14.1–14.5	11.9–12.5	1.5–5.5	3.1–5.9	2.0–6.0	1.9–5.6	2.1–5.6
	(12.5)[b] [2.2][c]	(14.6) [0.6]	(15.1) [0.6]	(14.3) [0.9]	(12.2) [1.5]	(3.0) [33.5]	(4.1) [14.2]	(3.8) [19.9]	(3.5) [23.7]	(3.4) [22.1]
pH	8.1–8.2	7.9–7.9	7.6–7.7	7.4–7.5	7.8–7.8	7.8–8.7	8.6–8.9	8.5–8.9	8.1–8.4	8.3–8.5
	(8.1) [0.1]	(7.9) [0.2]	(7.6) [0.1]	(7.4) [0.1]	(7.8) [0.1]	(8.4) [1.9]	(8.8) [0.6]	(8.7) [0.6]	(8.3) [0.9]	(8.4) [0.8]
EC (µs cm⁻¹)	223.9–225.1	285.1–285.5	328.0–329.1	381.1–382.2	316.4–318.4	228.0–231.0	266.0–277.0	316.0–338.0	379.0–389.0	312.0–319.0
	(224.5) [0.1]	(285.3) [0.1]	(328.6) [0.1]	(381.7) [0.1]	(317.4) [0.1]	(229.4) [0.4]	(272.0) [0.7]	(329.8) [1.0]	(383.5) [0.6]	(315.2) [0.6]
[Ca²⁺] (mg L⁻¹)[d]	32.9–33.1	41.5–41.5	47.5–47.6	54.9–55.1	45.9–46.1	33.5–33.9	38.8–40.3	45.8–48.9	54.6–56.0	45.2–46.2
	(33.0) [0.1]	(41.5) [0.1]	(47.6) [0.1]	(55.0) [0.1]	(46.0) [0.2]	(33.7) [0.4]	(39.6) [0.6]	(47.7) [1.0]	(55.3) [0.6]	(45.7) [0.6]
[Mg²⁺] (mg L⁻¹)[d]	9.8–9.9	8.7–8.8	20.1–20.2	18.7–18.8	12.5–12.7	10.1–10.2	13.2–13.3	12.2–12.3	18.9–19.1	11.8–11.9
	(9.9) [0.1]	(8.7) [0.1]	(20.1) [0.1]	(18.8) [0.1]	(12.7) [0.1]	(10.2) [0.6]	(13.2) [0.6]	(12.2) [0.9]	(19.1) [0.5]	(11.9) [0.5]
[HCO₃⁻] (mg L⁻¹)[d]	128.7–129.4	167.2–167.5	194.3–195.0	227.7–228.4	187.0–188.2	131.3–133.2	155.2–162.1	186.7–200.6	226.4–232.7	184.2–188.6
	(129.1) [0.2]	(167.4) [0.1]	(194.6) [0.1]	(228.1) [0.1]	(187.6) [0.2]	(132.1) [0.4]	(159.1) [0.7]	(195.4) [1.1]	(229.2) [0.6]	(186.2) [0.6]
[SO₄²⁻] (mg L⁻¹)[d]	28.2–28.3	42.9–43.0	56.6–56.8	24.6–24.8	42.1–42.2	27.9–28.0	43.3–43.4	55.4–55.5	23.6–23.7	40.3–40.6
	(28.3) [0.1]	(42.9) [0.1]	(56.8) [0.1]	(24.7) [0.1]	(42.2) [0.1]	(27.9) [0.1]	(43.4) [0.1]	(55.5) [0.1]	(23.7) [0.1]	(40.5) [0.1]
[NO₃⁻] (mg L⁻¹)[e]	3.5–3.7	11.5–11.6	3.4–3.5	–	–	2.6–2.8	9.5–9.9	2.7–3.1	–	–
	(3.6) [0.1]	(11.6) [0.1]	(3.5) [0.1]			(2.7) [3.1]	(9.7) [9.1]	(3.0) [13.2]		
SI_C	0.1–0.2	0.1–0.2	0.1–0.1	0.1–0.1	0.1–0.1	0.1–0.6	0.6–0.9	0.7–1.0	0.5–0.7	0.4–0.7
	(0.2) [6.4]	(0.2) [7.5]	(0.1) [0.1]	(0.1) [8.6]	(0.1) [7.3]	(0.3) [12.9]	(0.8) [6.0]	(0.9) [9.9]	(0.6) [10.9]	(0.6) [10.5]
pCO₂ (Pa)	77–82	165–190	372–391	671–689	237–253	19–58	14–31	17–49	63–128	39–78
	(70) [2.2]	(173) [3.1]	(382) [1.9]	(676) [1.0]	(246) [1.4]	(34) [26.4]	(19) [14.8]	(26) [30.4]	(87) [18.4]	(54) [17.8]
DO (mg L⁻¹)	0.1–3.4	3.5–3.5	0.0–3.6	0.0–0.1	0.0–2.8	7.3–10.5	7.7–11.7	9.1–15.3	8.0–12.9	8.3–14.0
	(3.3) [9.4]	(3.5) [2.1]	(3.4) [8.8]	(0.1) [0.1]	(2.6) [21.0]	(8.3) [10.5]	(9.2) [19.8]	(11.8) [28.9]	(9.5) [22.8]	(10.0) [20.0]
DOC (mg L⁻¹)[e]	0.7–0.8	1.1–1.2	1.2–1.3	1.9–2.0	1.3–1.4	0.9–1.2	1.3–1.6	1.4–1.7	2.5–2.8	2.0–2.3
	(0.8) [0.1]	(1.2) [0.1]	(1.3) [0.1]	(2.0) [0.1]	(1.4) [0.1]	(1.1) [15.1]	(1.5) [17.2]	(1.6) [25.2]	(2.7) [17.9]	(2.1) [18.3]
POC (mg L⁻¹)[e]	0.5–0.6	0.5–0.6	0.8–0.9	1.2–1.3	0.8–0.9	0.8–0.9	0.9–1.2	1.0–1.4	2.0–2.4	1.0–1.3
	(0.5) [0.1]	(0.6) [0.1]	(0.8) [0.1]	(1.2) [0.1]	(0.8) [0.1]	(0.8) [17.5]	(1.0) [19.1]	(1.2) [39.3]	(2.2) [24.6]	(1.2) [20.9]
δ¹³C_DIC (‰)[e]	−4.0–3.3	−5.4–4.8	−4.4–4.2	−13.2–12.4	−9.3–8.9	−4.2–3.7	−4.3–3.7	−2.4–1.9	−11.7–11.2	−8.5–7.0
	(−3.6) [7.0]	(−5.2) [3.8]	(−4.3) [1.7]	(−12.7) [2.4]	(−9.2) [1.4]	(−3.9) [3.8]	(−4.0) [4.7]	(−2.2) [6.7]	(−11.5) [1.4]	(−7.9) [6.5]
Q (L min⁻¹)	0.2	0.1	0.2	0.1	0.1	0.2	0.1	0.2	0.1	0.1

The mean values of the other ions: [K⁺] = 1.5 mg L⁻¹, [Na⁺] = 1.2 mg L⁻¹, [Cl⁻] = 0.3 mg L⁻¹, [PO₄³⁻]: lower than the detection limit.
[a] Minimum-maximum.
[b] Mean values, number of samples are 192.
[c] CV or variation coefficients = (standard deviation / mean) %.
[d] Calculated values via Equations.
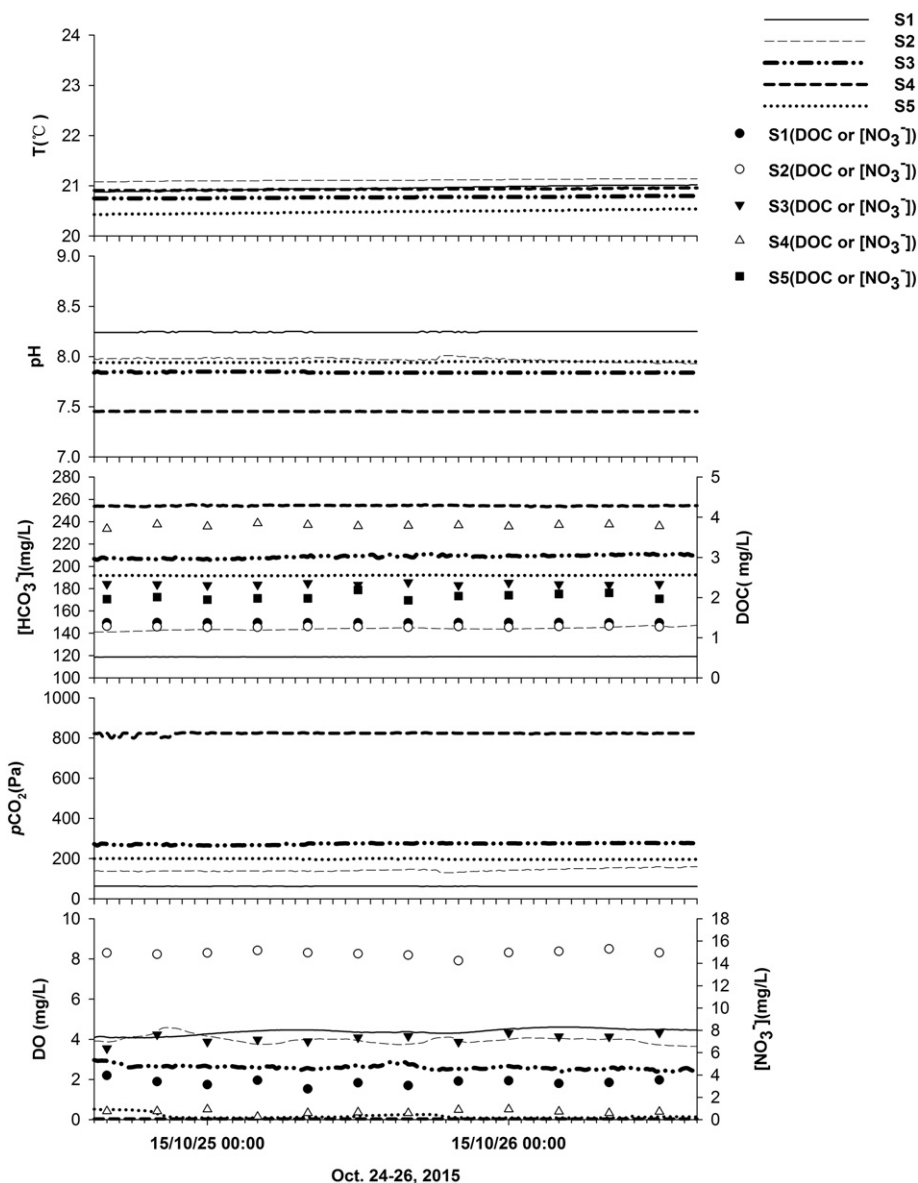[e] Sample analyzed value, number of samples are 12.

Fig. 2. Diurnal variations of the physical–chemical parameters of the five springs (S1 to S5) in autumn (October) (2-sigma error bars are smaller than the symbols). Notes: The pCO_2 is calculated.

noon), resulting in positive daily mean fluxes of 351.8 mg m^{-2} h^{-1} for P1 and 223.8 mg m^{-2} h^{-1} for P2. The other three ponds showed much stronger influxes at noon, thus leading to the negative daily mean fluxes. However in the winter season when plants are dormant, the spatial differences of CO_2 gas exchanges among these ponds are less apparent.

4.3. Variations of $\delta^{13}C_{DIC}$ in the spring-pond systems

The $\delta^{13}C_{DIC}$ variations in the two seasons are presented in Fig. 6 and Tables 2 and 3. Results show that there was no discernible diurnal variation of $\delta^{13}C_{DIC}$ in the spring water (with the CV values < 7.6% and 7.0% in autumn and winter, respectively). In addition, the seasonal difference of $\delta^{13}C_{DIC}$ in each spring was absent except for S4. The $\delta^{13}C_{DIC}$ values in S4 in October (−15.7‰ to −15‰) were more negative than those in January (−13.2‰ to −12.4‰). $\delta^{13}C_{DIC}$ in S4 has the most negative value, followed by S5 (−9.5‰ to −8.9‰ in October and −9.3‰ to −8.9‰ in January). The $\delta^{13}C_{DIC}$ of S1, S2 and S3 were similar to each other, with a range from −5.4‰ to −2.2‰.

In contrast, pronounced diurnal cycles were observed in the spring-fed ponds in autumn. The $\delta^{13}C_{DIC}$ increased during the daytime and reached a maximum at 18:00 h, then continuously decreased, approaching the minimum at 04:00 h. In winter, however, the daily cycles of $\delta^{13}C_{DIC}$ in the ponds were not apparent, with the CVs < 6.7%. Considering that the ponds inherited the characteristics of the springs, the seasonal differences of $\delta^{13}C_{DIC}$ in the spring-fed ponds are not so notable except for P4, where the $\delta^{13}C_{DIC}$ value was more negative in October (−14.7‰ to −13.4‰) than in January (−11.7‰ to −11.2‰). Spatially, the $\delta^{13}C_{DIC}$ value of P4 was the most negative, the next was P5 (−8.7‰ to −6.6‰ in October and −8.5‰ to −7‰ in January). The values of $\delta^{13}C_{DIC}$ of P1, P2 and P3 ranged from −4.8‰ to −1.6‰.

5. Discussion

5.1. Mechanisms causing the temporal variations in hydrochemistry, CO_2 fluxes and DIC isotopes in the pond waters: role of aquatic metabolism

It was found that all parameters in the spring water samples, including T, pH, ion concentrations, SI$_C$, pCO_2, DO and $\delta^{13}C_{DIC}$, showed no
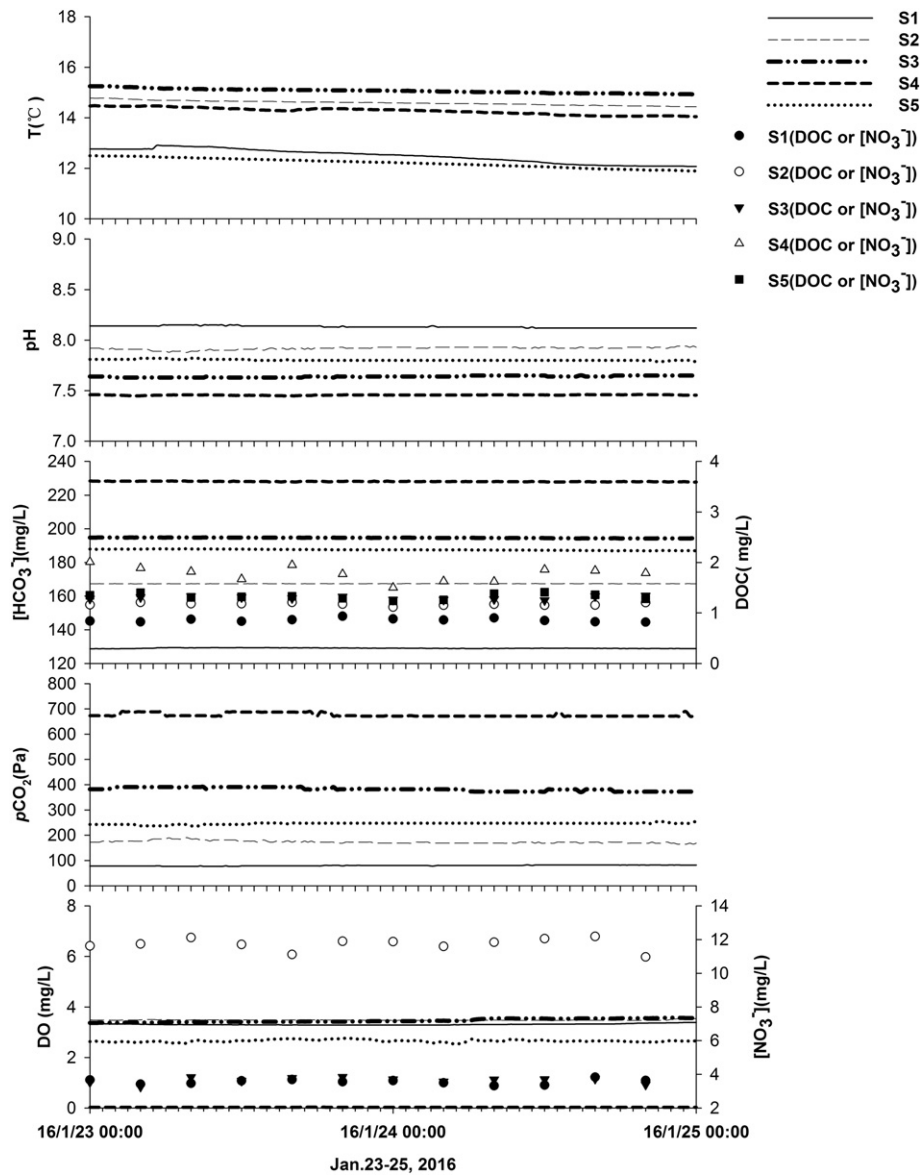
Fig. 3. The diurnal variations of the physical–chemical parameters of the five springs (S1 to S5) in winter (January).
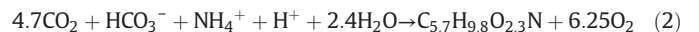
significant variations over the diurnal timescales (48 h) in both autumn and winter. This implies a large volume and well-mixed groundwater in the tanks. Thus, it can be safely assumed that the variations in hydrochemistry and carbon isotopic composition in pond water are attributed to biogeochemical processes rather than only inheriting the variability in those parameters in the source spring water.

However, the parameters do show differences on seasonal scales in the spring waters, especially at spring S4. Because CO_2 in groundwater generally originates from downward diffusion of soil CO_2 (Yang et al., 2012), the seasonal productivity of soil CO_2 that is mainly related to temperature and biological activity could be the primary reason for the seasonal differences of pCO_2 in the spring waters. In autumn, the higher temperature and biological activity lead to stronger root respiration and microbial activity, with the consequent higher production of soil CO_2, and thus increasing the concentration of HCO_3^- and decreasing the $\delta^{13}C_{DIC}$ values in the underlying groundwater (Fig. 6).

In contrast to the spring waters, almost all parameters displayed apparent diurnal cycles in the pond waters in the autumn (Figs. 4–6). Water temperature, pH and DO increased during the daytime and decreased at night, while $[HCO_3^-]$ and pCO_2 showed the opposite trends.

explained by the temperature-dependence of gas solubility, which should result in a negative rather than a positive correlation observed between DO and T (Table 5). The coupled variations in all parameters reflect significant control by aquatic biological metabolism. During the daytime, the photosynthesis of aquatic plants consumes CO_2 in the water and produces O_2, while respiration consumes dissolved O_2 and produces CO_2 at night. This is evidenced by the significant negative correlation between pCO_2 and DO in the pond water (Fig. 7 and Table 5). The data suggest that pCO_2 varies due to photosynthesis and respiration of aquatic plants, and pH shows the reverse trends, as expected (Figs. 4 and 5).

It is known that nitrogen (N) is one of the nutrients for photosynthesis. Participation of N into photosynthesis can be described in the following equations (Gammons et al., 2011):

$$5.7CO_2 + NO_3^- + H^+ + 4.4H_2O \rightarrow C_{5.7}H_{9.8}O_{2.3}N + 8.25O_2 \qquad (1)$$

$$4.7CO_2 + HCO_3^- + NH_4^+ + H^+ + 2.4H_2O \rightarrow C_{5.7}H_{9.8}O_{2.3}N + 6.25O_2 \qquad (2)$$

According to Eqs. (1) and (2), the concentration of N species correlates positively with pCO_2 and negatively with DO. In this study, positive
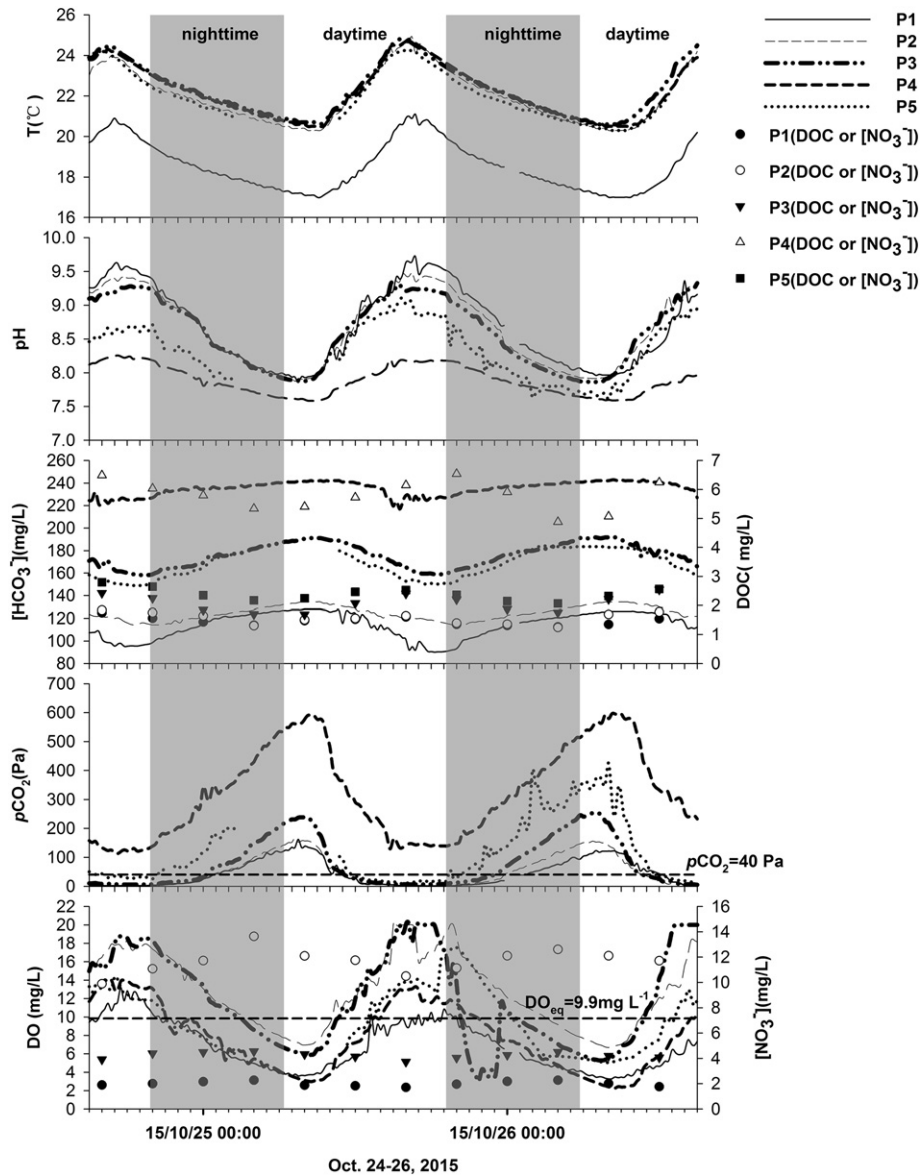
Fig. 4. Diurnal variations of the physical–chemical parameters of the five spring-fed ponds (P1 to P5) in the month representing autumn (October) (2-sigma error bars are smaller than the symbols).

correlations between [NO$_3^-$] and Δ[DIC] (the [DIC] difference between a spring and the spring-fed pond) as well as negative correlations between [NO$_3^-$] and DO were observed in P1, P2 and P3 in autumn (Table 5). This suggests that DO, [NO$_3^-$] and [DIC] variations in the pond waters were mainly due to aquatic community activity, and thus predominantly controlled by biological processes (Fig. 8). The concentrations of NO$_3^-$ in S4, S5, P4 and P5 are below the limits of detection, implying that the N species may be utilized thoroughly by the overlying vegetation and N-leaching was thus not available.

Stable carbon isotope composition (δ^{13}C) can be used to trace carbon sources or bio-geochemical processes (Han et al., 2010). The δ^{13}C$_{DIC}$ value in an aquatic ecosystem is determined by a balance between the effects of photosynthesis, respiration, gas exchange, groundwater contributions, and carbonate mineral precipitation or dissolution reactions. CO$_2$ degassing can cause an enrichment of δ^{13}C$_{DIC}$ in the residual DIC in streams. Some studies documented shifts in δ^{13}C$_{DIC}$ of up to 5‰ as a result of CO$_2$ degassing in a karst headwater stream within 0.5 km (Doctor et al., 2008). However, CO$_2$ degassing would be limited under slow flow rate conditions of the ponds water. Furthermore, pCO$_2$ of the ponds

(except for P4) were lower than atmosphere during daytime when aquatic photosynthesis was strong, indicating that aquatic metabolism had a more dominant influence on δ^{13}C$_{DIC}$ than degassing in ponds. Previous studies also have shown that δ^{13}C$_{DIC}$ values are strongly related to photosynthesis and respiration of aquatic plants, especially in a still water environment (Liu et al., 2006, 2015). During photosynthesis, ^{12}CO$_2$ is preferentially utilized, leading to an increase in δ^{13}C$_{DIC}$ values. In contrast, CO$_2$ released by respiration has an isotopic signature similar to that of the indigenous vegetation, which is depleted in ^{13}C such that δ^{13}C$_{DIC}$ value should be expected to decrease during night. Such periodic cycles were also observed in all five ponds in our study, but with the more remarkable trends in the autumn (Fig. 6). Thus the diurnal variation of δ^{13}C$_{DIC}$ provides another piece of evidence for control by aquatic plants on the hydrochemistry in these aquatic ecosystems.

Most streams and rivers have partial pressures of CO$_2$ (pCO$_2$) that are higher than those in equilibrium with the atmosphere (~40 Pa), implying that they also act as a source of atmospheric CO$_2$ via degassing (Singh et al., 2005; Hagedorn and Cartwright, 2009, 2010). Butman
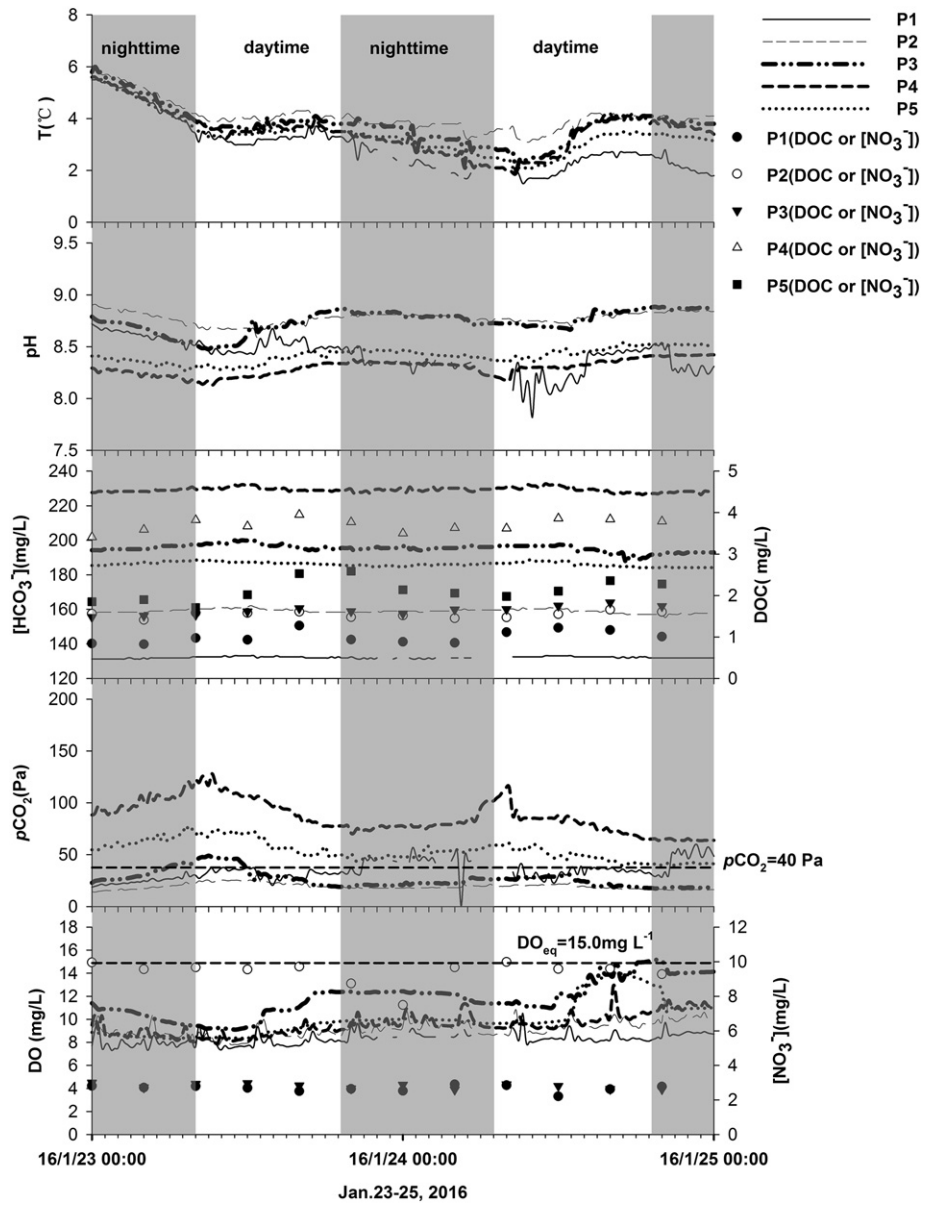
Fig. 5. Diurnal variations of the physical–chemical parameters of the five spring-fed ponds (P1 to P5) in the month representing winter (January).

and Raymond (2011) also indicated that inland streams and rivers tend to be supersaturated with respect to the standard atmosphere and thus are a net source of CO_2 to it. Further, Khadka et al. (2014) estimated that the pCO_2 of a karst river water can be as great as ×105 supersaturated with respect to the atmosphere. However, it is very interesting that pCO_2 values in our experimental pond waters were almost zero in the afternoon when photosynthesis was the strongest. This implies there was a flux of CO_2 from the atmosphere to the water, which is corroborated by the results from floating chamber test (Table 4). This

phenomenon suggests that strong aquatic photosynthesis in terrestrial surface waters might form another important natural carbon sink by drawing CO_2 directly from the atmosphere, as occurs in the oceans (Ducklow et al., 2001; Passow and Carlson, 2012).

During noon to early afternoon, the strong aquatic photosynthesis (with high DO concentration as indicator) corresponded to low pCO_2 levels which were <100 Pa except for P4 (Fig. 4). The CO_2 in the chamber was lower than that of the atmosphere (around 40 Pa), suggesting that there was CO_2 influx from the atmosphere to water instead

Table 4
Calculated CO_2 flux (F) in the spring-fed ponds in the autumn month (October) and the winter month (January).

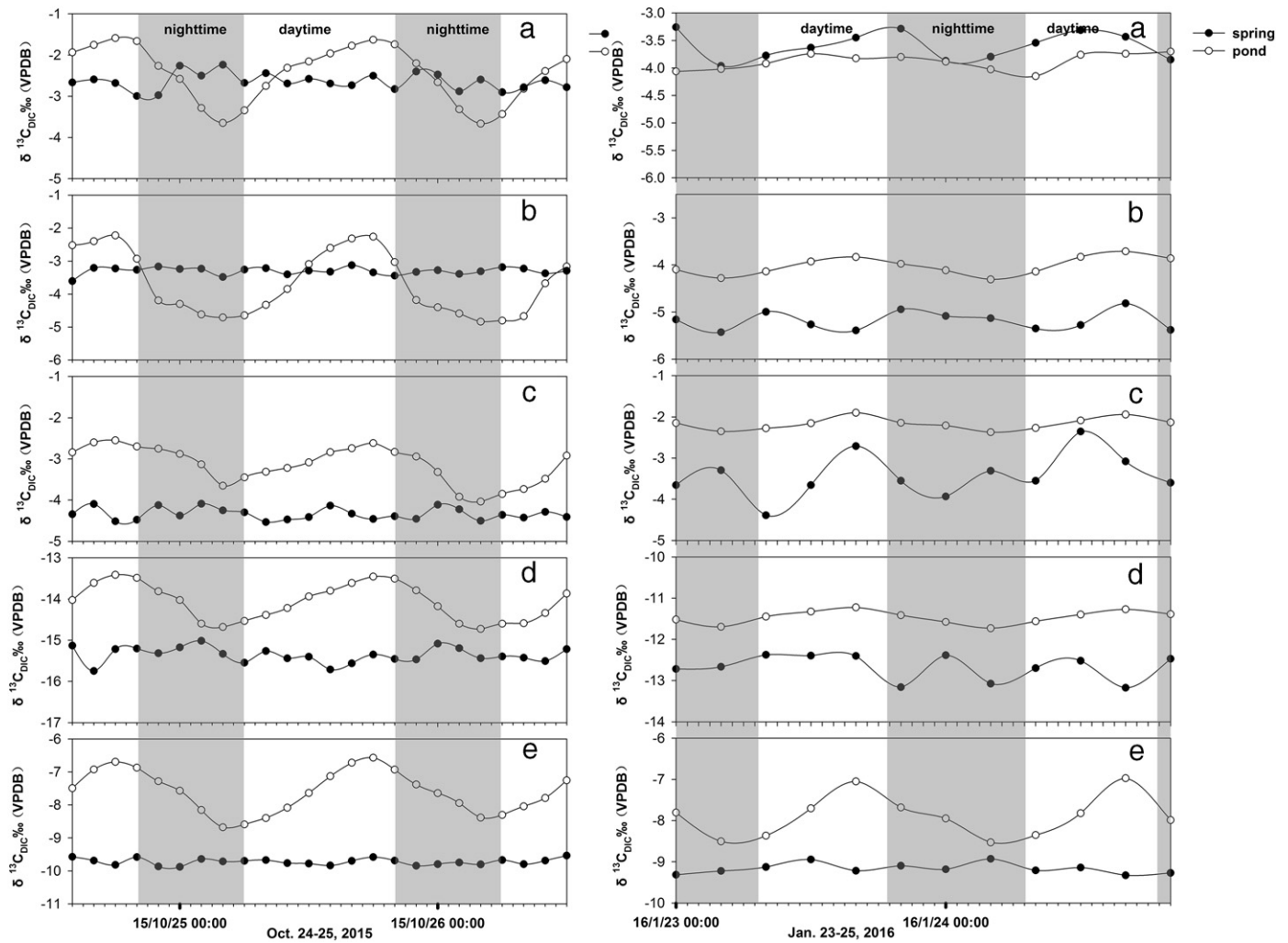| Site	P1		P2		P3		P4		P5	
Month	October	January	October	January	October	January	October	January	October	January
F-morning (mg m^{-2} h^{-1})	43	14	33	18	43	20	24	15	24	14
F-noon (mg m^{-2} h^{-1})	−28	−4	−30	−8	−84	−7	−45	−8	−79	−10
F-evening (mg m^{-2} h^{-1})	29	3	25	5	23	6	16	5	18	4
F-daily mean (mg m^{-2} d^{-1})	352	105	224	122	−146	146	−41	99	−303	65

Fig. 6. A comparison of diurnal variations in $\delta^{13}C_{DIC}$ of the five springs (S1 to S5) and the spring-fed ponds (P1 to P5) in autumn (left) and winter (right) (2-sigma error bars are smaller than the symbols) (a: LUCC1-S1-P1; b: LUCC2-S2-P2; c: LUCC3-S3-P3; d: LUCC4-S4-P4; e: LUCC5-S5-P5).

of CO_2 degassing. Table 4 displays the CO_2 flux of floating chamber in the five ponds. The daily mean of CO_2 flux in P5 was about -302.5 mg m^{-2} d^{-1}, which is twice of that in P3 and seven times of that in P4. P1 and P2 show a daily CO_2 degassing (positive flux) during

the day due to stronger organic decomposition and respiration than aquatic photosynthesis. From the regression equation in Fig. 9, one may obtain each CO_2 flux from the corresponding record of DO, and quantify the BCP effect.

Table 5
Correlations of DO versus T, pCO_2 and $\triangle pCO_2$ versus DO as well as DO and DIC versus [NO_3^-] in the spring-fed ponds in the autumn month (October) and the winter month (January).

Site		P1		P2		P3		P4		P5	
Month		October	January	October	January	October	January	October	January	October	January
DO vs T	Pearson correlation	0.917**	−0.438**	0.937**	−0.113	0.860**	−0.074	0.956**	−0.152*	0.955**	−0.261**
	Sig. (2-tailed)	0.000	0.000	0.000	0.000	0.000	0.000	0.000	0.000	0.000	0.000
	N	192	192	192	192	192	192	192	192	192	192
pCO_2 vs DO	Pearson correlation	−0.851**	0.120	−0.887**	−0.506**	−0.752**	−0.857**	−0.969**	−0.793**	−0.733**	−0.761**
	Sig. (2-tailed)	0.000	0.000	0.000	0.000	0.000	0.000	0.000	0.000	0.000	0.000
	N	192	192	192	192	192	192	192	192	192	192
$\triangle pCO_2$ vs DO	Pearson correlation	0.852**	−0.353**	0.859**	−0.326**	0.749**	0.299**	0.967**	0.640**	0.731**	0.735**
	Sig. (2-tailed)	0.000	0.000	0.000	0.000	0.000	0.000	0.000	0.000	0.000	0.000
	N	192	192	192	192	192	192	192	192	192	192
DO vs [NO_3^-]	Pearson correlation	−0.924**	−0.059	−0.871**	−0.375	−0.794**	−0.680*	–	–	–	–
	Sig. (2-tailed)	0.000	0.000	0.000	0.000	0.000	0.000				
	N	12	12	12	12	12	12				
$\triangle$DIC vs [NO_3^-]	Pearson correlation	0.685**	−0.252	0.742**	−0.016	0.761**	0.193	–	–	–	–
	Sig. (2-tailed)	0.000	0.000	0.000	0.000	0.000	0.000				
	N	12	12	12	12	12	12				

** Correlation is significant at the 0.01 level (2-tailed).
* Correlation is significant at the 0.05 level (2-tailed).

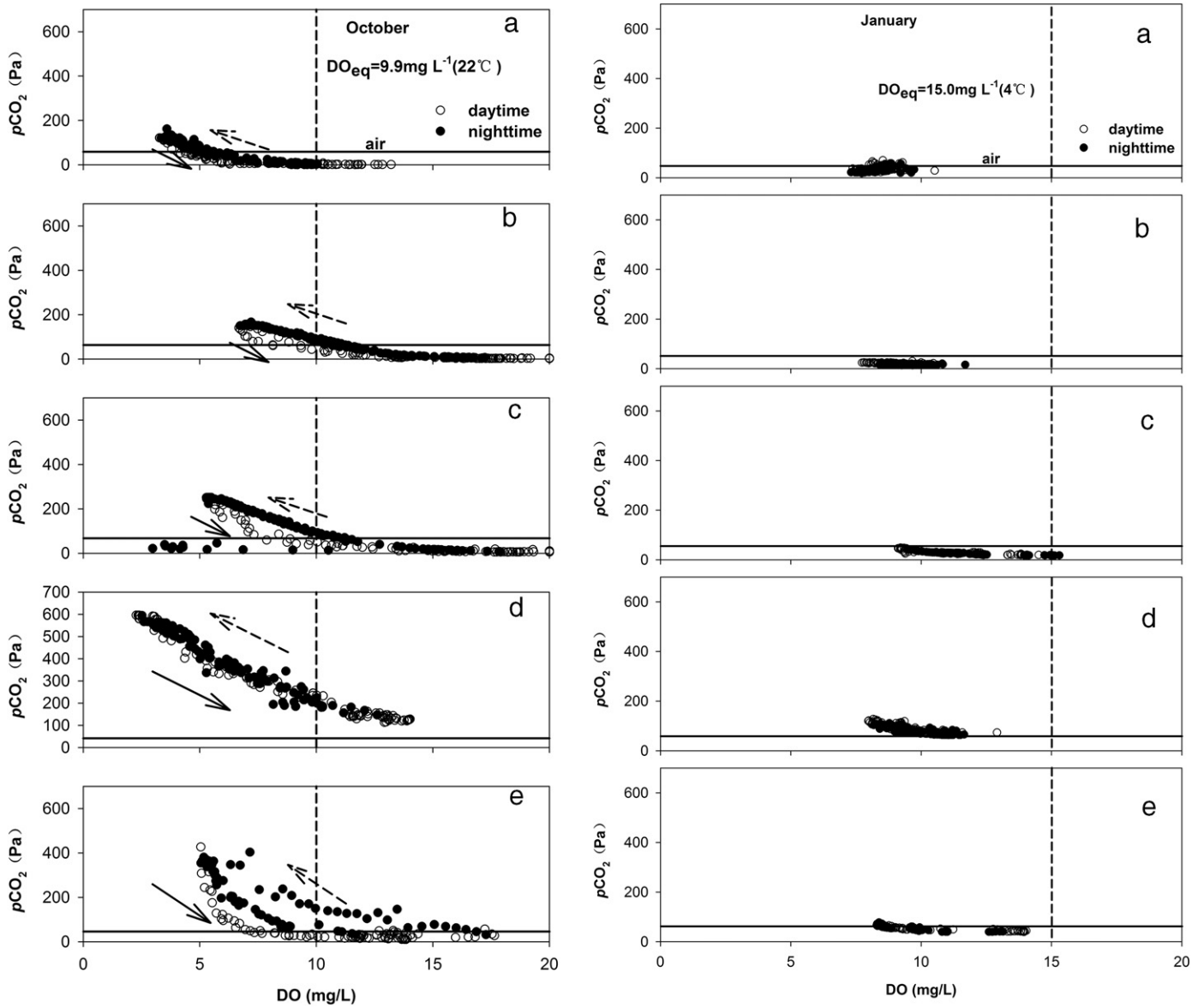**Fig. 7.** Cross-plots for pCO_2 and DO of the five spring-fed ponds (a: P1; b: P2; c: P3; d: P4; e: P5) in autumn (October) (left) and winter (January) (right). Solid arrows represent the trend of changes during the daytime and dashed arrows represent the trend of changes at night.

5.2. Mechanisms for the spatial variations in hydrochemistry, CO_2 fluxes and DIC isotopes of the pond waters: role of land use-related carbonate weathering

Figs. 2 to 6 show the hydrochemical parameters and $\delta^{13}C_{DIC}$ variations of the five springs and spring-fed ponds. The well-developed grass (LUCC4) intensified the root respiration and thus increased soil CO_2 concentration. The pCO_2 in spring S4 was the highest (mean value reaching 823 Pa in autumn and 676 Pa in winter), while the spring's DO was the lowest (0.04 mg L^{-1}). Except for pCO_2, [HCO$_3^-$], [NO$_3^-$] and $\delta^{13}C_{DIC}$ were also different due to the difference in land cover. The mean value of $\delta^{13}C_{DIC}$ in S4 was $-15‰$, while those for S1, S2 and S3 were around $-4‰$, indicating that soil respiration in tanks LUCC1 to LUCC3 was much weaker than in tank LUCC4. The $\delta^{13}C_{DIC}$ in S5 fell between S1 and S4, with an average value of $-9‰$.

It was found that Spirogyra and Hornwort were the dominant aquatic plants in ponds P2 and P3, Charophyta and Hydrilla in ponds P4 and P5, and only Spirogyra in pond P1. The CV of DO in P4 was the highest at 45.7%, implying the aquatic metabolism in P4 was the most intensive of the five ponds.

5.3. Quantifying the aquatic biological carbon pump effect

The decrease in DIC values in the ponds results from the joint effects of calcite precipitation, CO_2 exchange with the atmosphere, and DIC utilization by aquatic photosynthesis (Liu et al., 2015). DIC includes HCO$_3^-$, CO$_3^{2-}$ and CO_2 (aq). The proportions of these components depend on the pH values. In this study, where pH values range between 7.4 and 9.7, HCO$_3^-$ is the dominated component (84%–96%). Thus, the HCO$_3^-$ (Tables 2 and 3) is used as an approximation of DIC for this study. In addition, we used the decrease in [Ca^{2+}] (Tables 2 and 3) to predict calcite precipitation, and the fluxes of CO_2 (Table 4) in the five spring-fed ponds to estimate the CO_2 exchange with the atmosphere. The daily organic carbon formation in the ponds can then be estimated as follows:

$$M_{OC} = \int \left(\frac{[DIC]_{in} - [DIC]_{out}}{5.08}\right)_t Qdt - \int \left(\frac{[Ca]_{in} - [Ca]_{out}}{3.337}\right)_t \quad (3)$$

$$Qdt - \int \left(\frac{F}{3.664}\right)_t Adt \int \left(\frac{F}{3.664}\right)_t Adt - \int ([TOC]_s)_t Qdt$$
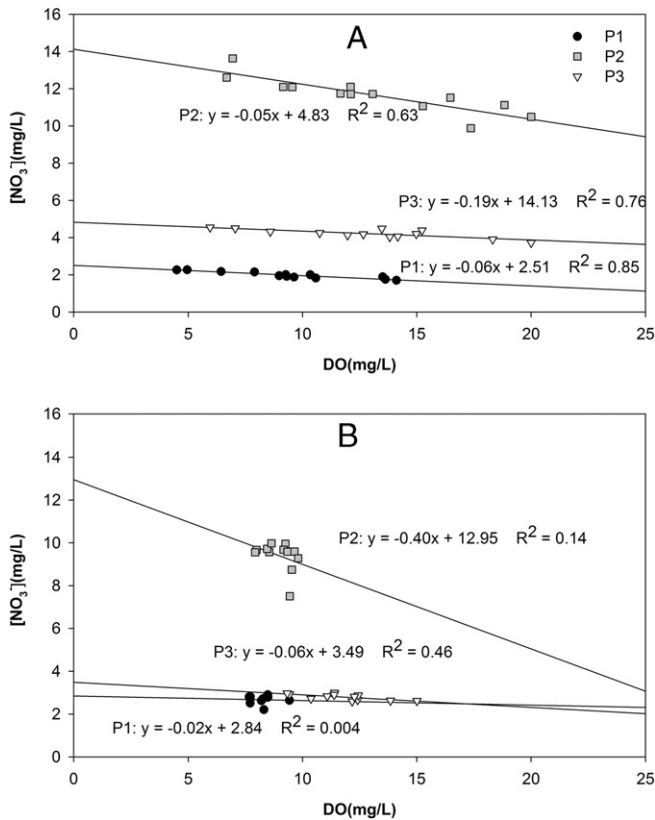
Fig. 8. Measured $[NO_3^-]$ versus DO of the spring-fed ponds (P1 to P3) in autumn (A) and winter (B).

where M_{OC} is the mass of organic carbon formed in one day (mg d^{-1}); Q is the flow rate of the pond; $[DIC]_s$ and $[DIC]_p$ are the HCO$_3^-$ concentrations (mg L^{-1}) at the spring and outlet of the ponds; 5.08 is the conversion factor between the molar mass of HCO$_3^-$ and carbon; $[Ca]_s$ and $[Ca]_p$

Fig. 9. Measured CO$_2$ fluxes (F_{CO2}) versus DO of the five spring-fed ponds (P1 to P5) in autumn (A) and winter (B).

are the Ca^{2+} concentrations (mg L^{-1}) at the spring and the outlet of the pond respectively; 3.337 is the conversion factor between the molar mass of calcium and carbon; F is the CO$_2$ flux from water surface (mg m^{-2} s^{-1}) and 3.664 is the conversion factor between the molar mass of CO$_2$ and carbon; A is the area of pond water surface (m^2) and $[TOC]_s$ and $[TOC]_p$ are the TOC concentrations (mg L^{-1}) at the spring and outlet of the ponds. The first term denotes the dissolved inorganic carbon loss/gain in a pond in a day; the second term is the amount of carbon deposited as calcite in a pond in a day; and the third term is the carbon loss/gain via CO$_2$ exchange in a pond in a day. In this study, dt is 15 min (the automatic recording interval).

From Eq. (3), in the autumn conditions the organic carbon sinks formed by submerged plants in the spring-fed ponds P1 through P5 were calculated to be 0.64 ± 0.21, 0.98 ± 0.34, 1.70 ± 0.57, 2.03 ± 0.68, and 1.64 ± 0.51 g d^{-1} (Fig. 10), respectively. This corresponds to fluxes of 156 ± 51, 239 ± 83, 414 ± 139, 493 ± 165 and 399 ± 124 t C km^{-2} a^{-1} in P1 to P5, respectively. These values are about 31 to 99 times higher than the marine BCP effect (Ducklow et al., 2001). This suggests a potentially significant role played by terrestrial aquatic photosynthesis in stabilizing the carbon sink by means of carbonate weathering and/or uptake of CO$_2$ directly from the atmosphere overhead. All these indicate the important role of terrestrial aquatic photosynthesis in stabilizing the carbon sink by carbonate weathering (HCO$_3^-$ to organic carbon) (Table 6).

The organic carbon production of the five spring-fed ponds, P1 through P5, in the winter were determined to be -0.14 ± 0.08, -0.23 ± 0.16, -0.29 ± 0.18, -0.21 ± 0.15, and -0.10 ± 0.07 g d^{-1}, respectively, corresponding to fluxes of -34 ± 20, -57 ± 38, -70 ± 45, -52 ± 37 and -25 ± 17 t C km^{-2} a^{-1} in P1 through P5, respectively (Table 4).

The seasonal difference in the organic carbon production suggest that, due to stronger light intensity, higher water temperatures, and higher spring DIC concentration (originating from higher content of soil CO$_2$) (Liu et al., 2007) in autumn, the organic carbon fluxes are positive. This implies storage of organic carbon in the ponds. In contrast, in winter, the aquatic photosynthesis was significantly limited because of weak light intensity and lower temperature. Also in the winter, the decomposition of sedimentary organic matter resulted in negative organic fluxes, where organic carbon was lost from the ponds.

5.4. DIC fertilization in the aquatic biological carbon sink: the role of different land uses

In autumn, there were different BCP effects among the five spring-fed ponds. This may be related to the combined effects of light intensity, temperature and DIC concentration, which determine the BCP strength. In general, increase in light intensity and temperature promote photosynthesis, while rising temperature also increases respiration (Staehr and Sand-Jensen, 2006). The increase in DIC concentration may accelerate the growth of algae, which is DIC fertilization effect (Z. Liu et al., 2010; Suarez-Alvarez et al., 2012; Yang et al., 2016).

In the autumn study month (October), the amount of organic carbon (M_{OC}) formed by aquatic plants in the spring-fed ponds differed in this order: P4 > P3 > P5 > P2 > P1 (Table 6). This is consistent with the DIC concentration order in the five spring-fed ponds. Moreover, M_{OC} showed a positive correlation with DIC ($R^2 = 0.97$, p < 0.0001, N = 5). The correlation shows that when the concentration of DIC in the ponds increased by 1 mg L^{-1}, the organic carbon produced by aquatic photosynthesis would increase by 2.5 t C km^{-2} a^{-1}. This shows the DIC fertilization effect in the karst aquatic ecosystem. Further, the role of aquatic photosynthesis in stabilizing DIC as the carbon sink may be more significant due to the higher DIC concentration in karst freshwater ecosystem than others.
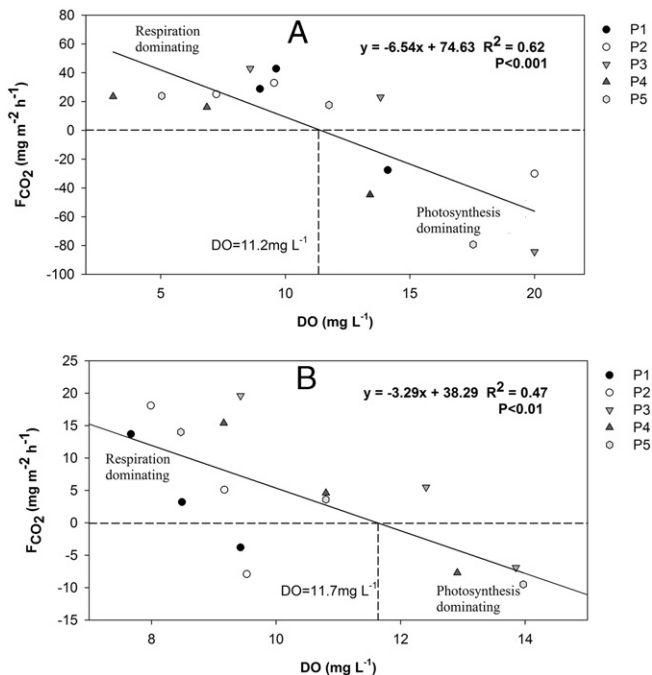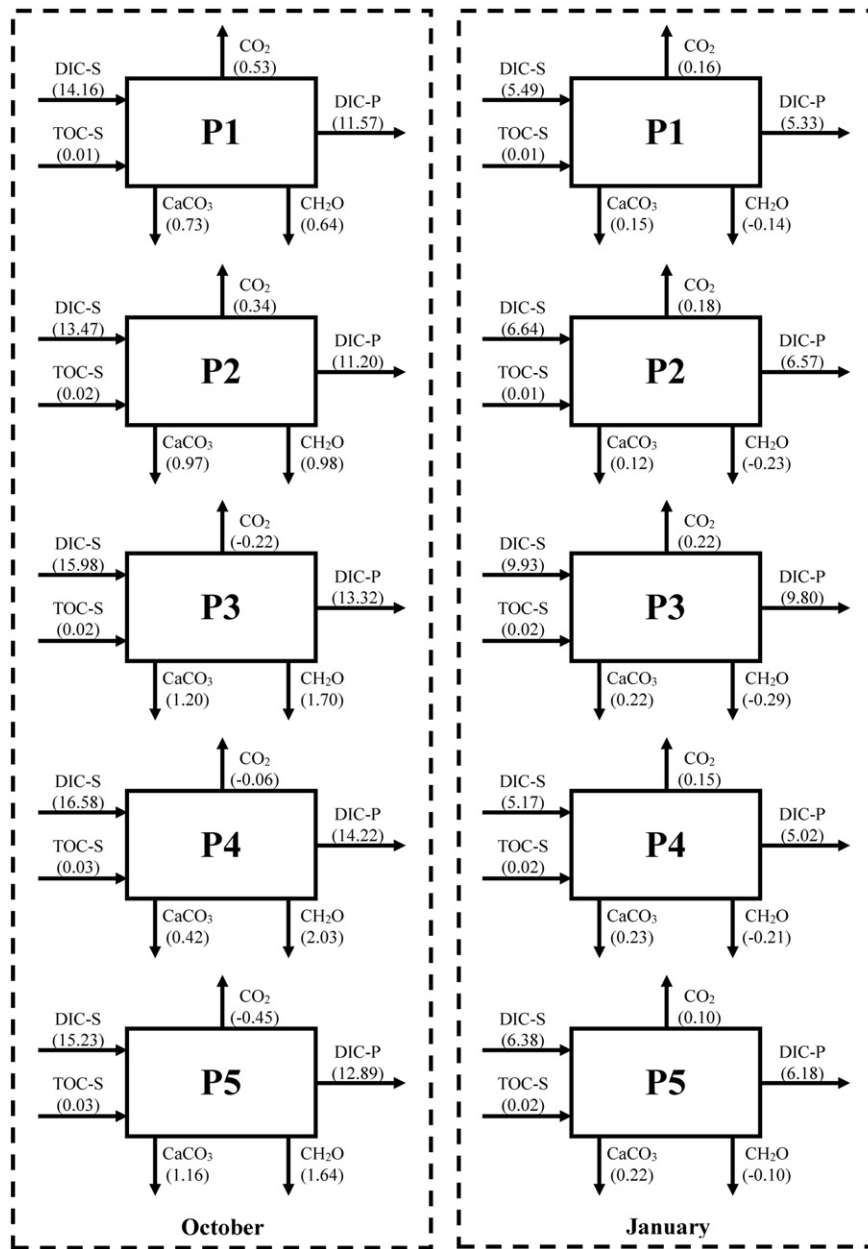
Fig. 10. Daily transport, transfer and mass balance of carbon ($g\ d^{-1}$) in the five spring-fedpond systems (P1 to P5) in winter (left) and autumn (right).

5.5. Implications for the carbon sink associated with rock weathering

Our research results have shown that ecosystem production and respiration and associated carbonate precipitation are the dominant processes influencing DIC in the experimental ponds. Daytime depletion of CO_2 due to photosynthesis resulted in calcite precipitation but CO_2 production from respiration at night was insufficient to induce significant carbonate dissolution. DIC entering the ponds from springs, a by-product of the chemical weathering of the limestone rubble, was promoted by soil respiration. Further, strong aquatic photosynthesis in terrestrial surface waters might constitute another important natural carbon sink by drawing CO_2 directly from the atmosphere, as in the oceans (Ducklow et al., 2001; Passow and Carlson, 2012). When the biological carbon pumping effect was strong enough, as with a sunny weather in the autumn, there was even an influx from air to water, showing the importance of underwater photosynthesis in both stabilizing the carbon sink (as DIC) by carbonate dissolution and creating new carbon sink directly from atmosphere. In summary, with the changing

climate and ecological systems, the link between dissolution and precipitation within carbonate areas may be altered, leading to a net influence on the local or global carbon cycles (Martin et al., 2013).

The different land uses and land covers created variety in the spring input waters which determined the initial conditions, including DIC and nutrient concentration. These primary factors, especially the concentration of DIC, influenced the community composition of the aquatic ecosystem. The changes in OC production rates in the spring-fed ponds were more influenced by the intensity of vegetal activity under the different land uses, implying that the amount of autochthonous OC sequestered by aquatic photosynthesis was determined by the differences in land use. In other words, the concentration of DIC can be altered by changing the types of land use, and the BCP effect in terrestrial aquatic settings can be controlled and thus the role of inland aquatic ecosystems in the global carbon sink is enhanced. At the same time, the terrestrial BCP could be impacted by climate change, as discussed before. In summary, the rate of carbonate weathering and the terrestrial BCP effect could increase due to the rise of temperature, which would

Table 6
Comparison of CO_2 degassing to the atmosphere from some carbonate-dominated rivers (streams) in the world.

Site		Climate	F_{CO2} (t C km^{-2} a^{-1})	BCP effect (t C km^{-2} a^{-1})	DO (mg L^{-1})	Ref.
P1	(October)	Subtropical (sunny)	− 242[b]–375[b]	526 ± 172[b] to −91 ± 30[b]	9.1–3.6 (7.9 at 21 °C)[c]	This study
	(January)	Subtropical (cloudy)	−33–120	33 ± 20 to −120 ± 72	8.5–7.7 (11.1 at 6 °C)	This study
P2	(October)	Subtropical (sunny)	−264–289	585 ± 202–32 ± 11	20.0–7.0 (7.3 at 25 °C)	This study
	(January)	Subtropical (cloudy)	−69–159	57 ± 39 to −171 ± 117	9.2–8.0 (11.1 at 6 °C)	This study
P3	(October)	Subtropical (sunny)	−739–376	1099 ± 368 to −15 ± 5	20.0–6.0 (7.3 at 25 °C)	This study
	(January)	Subtropical (cloudy)	−61–171	43 ± 27,189 ± 120	12.2–9.4 (11.1 at 6 °C)	This study
P4	(October)	Subtropical (sunny)	−392–206	870 ± 292–272 ± 91	12.8–3.1(7.3 at 25 °C)	This study
	(January)	Subtropical (cloudy)	−67–135	51 ± 37 to −151 ± 110	9.4–8.0 (11.1 at 6 °C)	This study
P5	(October)	Subtropical (sunny)	−694–209	983 ± 306–79 ± 25	13.7–5.8 (7.4 at 24 °C)	This study
	(January)	Subtropical (cloudy)	−84–123	82 ± 57 to −125 ± 87	9.9–8.5 (11.1 at 6 °C)	This study
Maolan spring-ponds (summer)		Subtropical	−119–67	677 to −50	11.31–8.46(8.3 at 28 °C)	Liu et al., 2015
Maolan spring-ponds (autumn)		Subtropical	−42–47	892 ± 300 to −176 ± 62	12.3–5.54 (10.1 at 18 °C)	Yang et al., 2015
Maolan spring-ponds (winter)		Subtropical	−9–32	285 ± 193 to −60 ± 40	11.71–9.78 (11.5 at 12 °C)	Yang et al., 2015
Xijiang river		Subtropical	186–410	NA[a]	72–97%	Zhai et al., 2007
Changjiang river		Humid subtropical	830–1560	NA	NA	Yao et al., 2007
Santa Fe river		Subtropical	402–1156	NA	30–80%	Khadka et al., 2014

[a] Not available.
[b] Are the paired values with strong and weak BCP effects respectively.
[c] Theoretical value of DO equilibrated with atmospheric O_2 at elevation of 1100 m at the sampling site (http://www.fivecreeks.org/monitor/do.shtml).

provide a negative feedback mechanism to global warming in the future.

6. Conclusions

By constructing five karst spring-pond systems of the same size but with different vegetation covers, we were able to investigate diurnal hydrochemical variations in the ponds in two seasons, to demonstrate the effect of different land uses and aquatic biological processes on carbon cycle at a karst-analog test site.

Our results show that there was little or no diurnal variation in the five spring water physical and chemical parameters that were monitored. However, pronounced cyclic daily variations were observed in temperature, DO, pH, EC, HCO$_3^-$, NO$_3^-$, pCO$_2$, DOC, and $\delta^{13}C_{DIC}$ with different patterns and amplitudes of variation in the waters of the five spring-fed ponds. The temperature, pH, DO, DOC and $\delta^{13}C_{DIC}$ in the ponds increased during the day and decreased at night, while EC, [HCO$_3^-$], [NO$_3^-$] and pCO$_2$ decreased during the day and increased at night.

The large losses of DIC between the spring and pond outlets are mainly attributed to biological storage of carbon, demonstrating that natural surface waters may constitute an important carbon sink. This loss of DIC is at least partly transformed into OC by the BCP effect, the products of which were then buried as autochthonous organic matter. Moreover, if the BCP effect is strong enough, as in the case of ponds under optimum photosynthesis conditions, there is a net CO$_2$ sink directly from the atmosphere to the open waters. It was determined that the BCP products in the ponds were 156 ± 51 t C km^{-2} a^{-1} in P1(bare rocky land), 239 ± 83 t C km^{-2} a^{-1} in P2 (bare land), 414 ± 139 t C km^{-2} a^{-1} in P3 (cultivated land), 493 ± 165 t C km^{-2} a^{-1} in P4 (grassland), 399 ± 124 t C km^{-2} a^{-1} in P5 (brushland) in autumn, indicating a potential significant role of terrestrial aquatic photosynthesis in stabilizing the carbonate weathering-related carbon sink (from DIC to organic carbon) and/or uptake of CO$_2$ directly from the overlying atmosphere. In contrast, in winter the aquatic photosynthesis was significantly reduced due to the low light intensity and low temperature.

Finally, higher DIC results in more aquatic photosynthetic production, the "DIC fertilization effect". This indicates that carbon sequestration originating from water-carbonate rock-CO$_2$ gas-aquatic organism interaction can be regulated and enhanced by appropriate land use management, which show significant control on the DIC concentration. For example, there would be largest increase in carbonate weathering-related carbon sink with land use change from bare rocky land to grassland.

References

Butman, D., Raymond, P.A., 2011. Significant efflux of carbon dioxide from streams and rivers in the United States. Nat. Geosci. 4, 839–842.

Clarke, S.J., 2002. Vegetation growth in rivers: influences upon sediment and nutrient dynamics. Prog. Phys. Geogr. 26, 159–172.

Cole, J.J., Prairie, Y.T., Caraco, N.F., McDowell, W.H., Tranvik, L.J., Striegl, R.G., Duarte, C.M., Kortelainen, P., Downing, J.A., Middelburg, J.J., Melack, J., 2007. Plumbing the global carbon cycle: Integrating inland waters into the terrestrial carbon budget. Ecosystems 10, 172–185.

De Montety, V., Martin, J.B., Cohen, M.J., Foster, C., Kurz, M.J., 2011. Influence of diel biogeochemical cycles on carbonate equilibrium in a karst river. Chem. Geol. 283, 31–43.

Doctor, D.H., Kendall, C., Sebestyen, S.D., Shanley, J.B., Ohte, N., Boyer, E.W., 2008. Carbon isotope fractionation of dissolved inorganic carbon (DIC) due to outgassing of carbon dioxide from a headwater stream. Hydrol. Process. 22, 2410–2423.

Ducklow, H.W., Steinberg, D.K., Buesseler, K.O., 2001. Upper ocean carbon export and the biological pump. Oceanography 14, 50–58.

Gammons, C.H., Babcock, J.N., Parker, S.R., Poulson, S.R., 2011. Diel cycling and stable isotopes of dissolved oxygen, dissolved inorganic carbon, and nitrogenous species in a stream receiving treated municipal sewage. Chem. Geol. 283, 44–55.

Hagedorn, B., Cartwright, I., 2009. Climatic and lithologic controls on the temporal and spatial variability of CO$_2$ consumption via chemical weathering: an example from the Australian Victorian Alps. Chem. Geol. 260, 234–253.

Hagedorn, B., Cartwright, I., 2010. The CO$_2$ system in rivers of the Australian Victorian Alps: CO$_2$ evasion in relation to system metabolism and rock weathering on multiannual time scales. Appl. Geochem. 25, 881–899.

Han, G., Tang, Y., Wu, Q., 2010. Hydrochemistry and dissolved inorganic carbon isotopic composition on karst groundwater in Maolan, southwest China. Environ. Earth Sci. 60, 893–899.

Harrison, J.A., Matson, P.A., Fendorf, S.E., 2005. Effects of a diel oxygen cycle on nitrogen transformations and greenhouse gas emissions in a eutrophied subtropical stream. Aquat. Sci. 67, 308–315.

Heffernan, J.B., Cohen, M.J., 2010. Direct and indirect coupling of primary production and diel nitrate dynamics in a large spring-fed river. Limnol. Oceanogr. 55, 677–688.

Khadka, M., Martin, J., Jin, J., 2014. Transport of dissolved carbon and CO$_2$ degassing from a river system in a mixed silicate and carbonate catchment. J. Hydrol. 513, 391–402.

Kurz, M.J., de Montety, V., Martin, J.B., Cohen, M.J., Foster, C.R., 2013. Controls on diel metal cycles in a biologically productive carbonate-dominated river. Chem. Geol. 358, 61–74.

Liu, Z., Dreybrodt, W., 2015. Significance of the carbon sink produced by H$_2$O-carbonate-CO$_2$-aquatic phototroph interaction on land. Sci. Bull. 60, 182–191.

Liu, Z., Li, Q., Sun, H., Liao, C., Li, H., Wang, J., Wu, K., 2006. Diurnal variations of hydrochemistry in a travertine-depositing stream at Baishuitai, Yunnan, SW China. Aquat. Geochem. 12, 103–121.

Liu, Z., Li, Q., Sun, H., Wang, J., 2007. Seasonal, diurnal and storm-scale hydrochemical variations of typical epikarst spring in subtropical karst areas of SW China: soil CO$_2$ and dilution effects. J. Hydrol. 337, 207–223.

Liu, Z., Liu, X., Liao, C., 2008. Daytime deposition and nighttime dissolution of calcium carbonate controlled by submerged plants in a karst spring-fed pool: insights from high time-resolution monitoring of physico-chemistry of water. Environ. Geol. 55, 1159–1168.

Liu, Z., Dreybrodt, W., Wang, H., 2010. A new direction in effective accounting for the atmospheric CO_2 budget: considering the combined action of carbonate dissolution, the global water cycle and photosynthetic uptake of DIC by aquatic organisms. Earth-Sci. Rev. 99, 162–172.

Liu, Y., Liu, Z., Zhang, J., He, Y., Sun, H., 2010. Experimental study on the utilization of DIC by *Oocystis solitaria* Wittr and its influence on the precipitation of calcium carbonate in karst and non-karst waters. Carbonates Evaporites 25, 21–26.

Liu, H., Liu, Z., Macpherson, G.L., Yang, R., Chen, B., Sun, H., 2015. Diurnal hydrochemical variations in a karst spring and two ponds, Maolan Karst Experimental Site, China: biological pump effects. J. Hydrol. 522, 407–417.

Martin, J., Brown, A., Ezell, J., 2013. Do carbonate karst terrains affect the global carbon cycle? Acta Carsol. 42, 187–196.

Parker, S.R., Gammons, C.H., Poulson, S.R., DeGrandpre, M.D., 2007. Diel variations in stream chemistry and isotopic composition of dissolved inorganic carbon, upper Clark Fork River, Montana, USA. Appl. Geochem. 22, 1329–1343.

Parker, S.R., Gammons, C.H., Poulson, S.R., DeGrandpre, M.D., Weyer, C.L., Smith, M.G., Babcock, J.N., Oba, Y., 2010. Diel behavior of stable isotopes of dissolved oxygen and dissolved inorganic carbon in rivers over a range of trophic conditions, and in a mesocosm experiment. Chem. Geol. 269, 22–32.

Passow, U., Carlson, C.A., 2012. The biological pump in a high CO_2 world. Mar. Ecol. Prog. Ser. 470, 249–271.

Poulson, S.R., Sullivan, A.B., 2010. Assessment of diel chemical and isotopic techniques to investigate biogeochemical cycles in the upper Klamath River, Oregon, USA. Chem. Geol. 269, 3–11.

Schulz, M., Köhler, J., 2006. A simple model of phosphorus retention evoked by submerged macrophytes in lowland rivers. Hydrobiologia 563, 521–525.

Singh, S.K., Sarin, M.M., France-Lanord, C., 2005. Chemical erosion in the eastern Himalaya: major ion composition of the Brahmaputra and $\delta^{13}C$ of dissolved inorganic carbon. Geochim. Cosmochim. Acta 69, 3573–3588.

Spencer, R.G.M., Pellerin, B.A., Bergamaschi, B.A., Downing, B.D., Kraus, T.E.C., Smart, D.R., Dahlgren, R.A., Hernes, P.J., 2007. Diurnal variability in riverine dissolved organic matter composition determined by in situ optical measurements in the San Joaquin River (California, USA). Hydrol. Proc. 21, 3181–3189.

Staehr, P.A., Sand-Jensen, K.A.J., 2006. Seasonal changes in temperature and nutrient control of photosynthesis, respiration and growth of natural phytoplankton communities. Freshw. Biol. 51, 249–262.

Suarez-Alvarez, S., Gomez-Pinchetti, J., García-Reina, G., 2012. Effects of increased CO_2 levels on growth, photosynthesis, ammonium uptake and cell composition in the macroalga *Hypnea spinella* (Gigartinales, Rhodophyta). J. Appl. Phycol. 24, 815–823.

Suman, S., Singh, N.P., Sulekh, C., 2012. Effect of filter backwash water when blends with raw water on total organic carbon and dissolve organic carbon removal. Res. J. Chem. Sci. 2 (10), 38–42.

Sun, H., Han, J., Zhang, S., Lu, X., 2011. Transformation of dissolved inorganic carbon (DIC) into particulate organic carbon (POC) in the lower Xijiang River, SE China: an isotopic approach. Biogeosci. Discuss. 8, 9471–9501.

Waterson, E.J., Canuel, E.A., 2008. Sources of sedimentary organic matter in the Mississippi River and adjacent Gulf of Mexico as revealed by lipid biomarker and $\delta^{13}C_{TOC}$ analyses. Org. Geochem. 39, 422–439.

Yang, R., Liu, Z., Zeng, C., Zhao, M., 2012. Response of epikarst hydrochemical changes to soil CO_2 and weather conditions at Chenqi, Puding, SW China. J. Hydrol. 468, 151–158.

Yang, R., Chen, B., Liu, H., Liu, Z., Yan, H., 2015. Carbon sequestration and decreased CO_2 emission caused by terrestrial aquatic photosynthesis: insights from diurnal hydrochemical variations in an epikarst spring and two spring-fed ponds in different seasons. Appl. Geochem. 63, 248–260.

Yang, M., Liu, Z., Sun, H., Yang, R., Chen, B., 2016. Organic carbon source tracing and DIC fertilization effect in the Pearl River: insights from lipid biomarker and geochemical analysis. Appl. Geochem. 73, 132–141.

Yao, G., Gao, Q., Wang, Z., Huang, X., He, T., Zhang, Y., Jiao, S., Ding, J., 2007. Dynamics of CO_2 partial pressure and CO_2 outgassing in the lower reaches of the Xijiang River, a subtropical monsoon river in China. Sci. Total Environ. 376, 255–266.

Zhai, W., Dai, M., Guo, X., 2007. Carbonate system and CO_2 degassing fluxes in the inner estuary of Changjiang (Yangtze) River, China. Mar. Chem. 107, 342–356.